

Patient-specific modeling of the carotid arteries for surgical simulation

M. Natanzon¹, N. Broide¹, M. Freiman¹, E. Nammer², L. Weizman¹, O. Shilon², L. Joskowicz¹, J. Sosna³

¹The Hebrew University of Jerusalem, School of Eng. and Computer Science, Jerusalem, Israel

²Symbionix Ltd., Lod, Israel

³Hadassah Hebrew Univ. Medical Center, Dept. of Radiology, Jerusalem, Israel

Keywords Carotid arteries segmentation · Patient specific modeling · Surgical simulation

Purpose

Minimally invasive endovascular surgeries such as carotid, coronary, and cerebral angiographic procedures are frequent interventional radiology procedures. They call for percutaneously introducing a flexible catheter into a large blood vessel and advancing it until a target is reached under fluoroscopic X-ray guidance with an injected contrast agent. With the catheter in place, procedures are performed and implants are placed.

Endovascular procedures require experienced physicians and involve significant time-consuming trial and error with repeated contrast agent injection and X-ray imaging. This leads to outcome variability and non-negligible complication rates. The key difficulties are the inter-patient anatomy and pathology variations, the unpredictable behavior of the catheter and implants, the preoperative planning based on static 2D images, and the inability to visualize the expected intraoperative fluoroscopic images.

Training simulators such the ANGIO Mentor™ (Symbionix Ltd, Israel) simulation platform for interventional endovascular procedures (Fig. 1a) have the potential to significantly reduce the physicians' learning curve, reduce the outcome variability, and improve their performance. A key limitation is the simulators' reliance on hand-tailored anatomical models generated by a technician from the manual segmentation (Fig. 1b), which is impractical to produce patient-specific simulations in a clinical environment in a timely fashion.

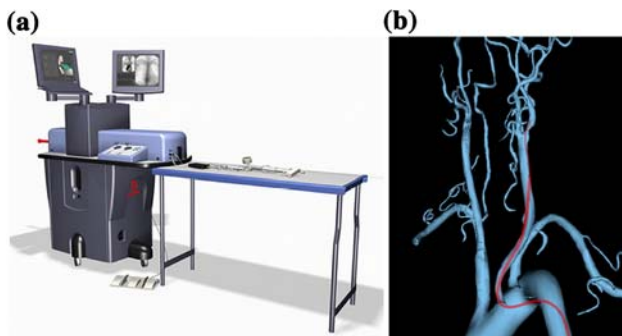


Fig. 1 (a) The Symbionix® Angio Mentor™ and (b) 3D visualization of a manually generated model of the carotid arteries (catheter shown in red)

We have developed a nearly automatic carotid arteries segmentation method to produce patient-specific simulation models from CT angiography (CTA). The task is challenging because of significant intra-patient carotid intensity variances, significant inter-patient carotid geometry and intensity variances, and intensity values overlap of the carotids and the neck vertebrae. Existing intensity-based, geometric shape, edge-based active contours and statistical active shape models algorithms struggle with these challenges [1].

Method

We have developed a carotid segmentation method which consists of three steps: (1) automatic aorta segmentation; (2) automatic carotid and vertebral, sub-clavian arteries segmentation, and; (3) nearly automatic user-driven segmentation refinement.

- (1) Aorta segmentation: We use morphological operators and prior anatomical knowledge of the aorta, including its location, estimated radius, and relative brightness, to segment the aorta. The aorta intensity values serve as the initial estimation of the arteries intensity distribution.
- (2) Arteries segmentation: We use a min-cut graph segmentation approach [2] to segment the arteries. We combine the estimated aorta intensity distribution, geometric tube-like shape priors based on multi-scale Hessian eigen-analysis [3], and local image gradients, into a graph-based image volume representation. In this graph, each node corresponds to a voxel and is connected by an edge to its neighboring voxels and two special 'source' and 'target' terminal nodes. The edges between the voxel and the terminal nodes represent the probability that the voxel is related to the vessels (source) or to the background (target). Edges between voxels represent gradient strength between the voxels. We then compute the graph min-cut separating the arteries (foreground) from other tissues (background). To reduce the memory requirements, the algorithm automatically divides the image volume into several block regions based on the aorta information. The min-cut for each block is computed separately, and the results are merged together.
- (3) Nearly automatic refinement: inevitably, the arteries segmentation step may produce disconnected vessel segments or miss some small vessels altogether. To allow to user to easily fix them, we have developed a new, graph-based, interactive tool for robust vessels segmentation. The tool requires the user to identify two points for each defective or missing vessel and produces a segmentation of the vessel in two steps: vessel trajectory estimation and optimal vessel surface computation.

The vessel trajectory estimation step computes the shortest path between the user-defined points using a graph representation of the image volume as above. This time, the edge weights are a combination of image intensity differences, gradient directions, and overall Manhattan path length. Based on this path, the algorithm automatically estimates the vessel segment radius and defines an uncertainly region in which the vessel surface is located. The optimal vessel surface computation step computes the vessel surfaces with an active contour graph min-cut approach based on image intensity and

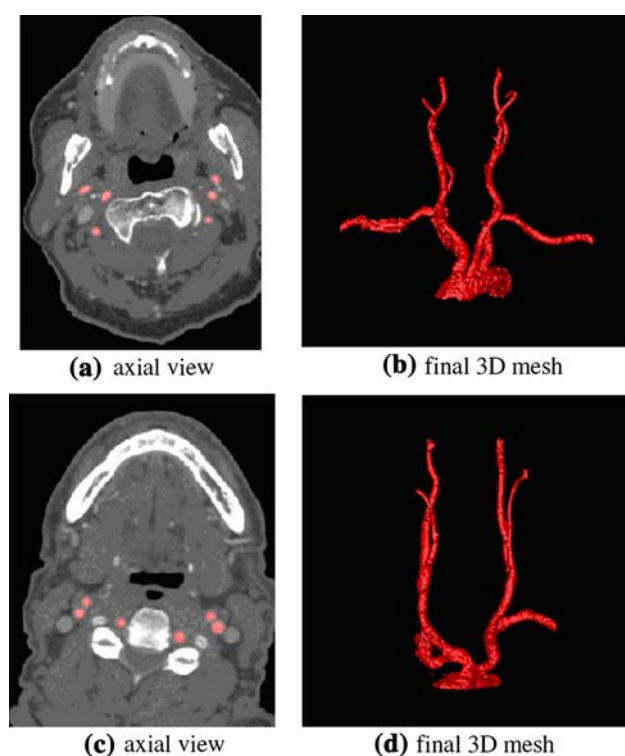


Fig. 2 (a) and (c) Automatic segmentation results (in red) overlaid on the original CTA images for two datasets. (b) and (d) 3D mesh visualization after interactive clean-up

gradient directions to ensure smooth vessel surfaces [4]. The physician refines the segmentation as desired, and the algorithm automatically generates the aorta and arteries meshes that are used in the simulation (Fig. 2).

Results

We evaluated the performance of our segmentation method on 30 carotid arteries vessels segments obtained from 15 clinical CTA datasets ($512 \times 512 \times 120\text{--}800$ voxels) on a standard PC (dual-core 32-bit 4 GHz 2 GB running Linux). Ground-truth segmentations and centerlines were obtained by manual segmentation and were verified and corrected by an expert radiologist. We measured our volume segmentation accuracy, compared to the ground-truth using the segmentation evaluation metrics in [5]. The average symmetric surface distance for 15 cases was 0.79 mm (STD = 0.25 mm), which is appropriate for the simulations. The automatic segmentation took on average 7:50 min for each high-resolution dataset and 2:34 min for each low-resolution dataset. The interactive refinement was used to remove veins and fix small discontinuities. It took at most one additional minute for each dataset.

Conclusion

We have developed a nearly automatic method for patient-specific modeling of the aorta and the carotid, vertebral, and sub-clavian arteries for patient-specific simulations from CTA images. The method automatically generates a vessels segmentation which is then refined with an easy-to-use tool to produce a mesh for simulation. Our results show that the proposed method is accurate, robust, easy to use, and can be integrated into existing simulators for patient-specific simulations.

We are currently integrating the algorithm in to the simulation platform and are extending it to other vascular structures, such as liver vessels and abdominal aortic aneurisms.

References

1. Kirbas, C. and Quek, F.K.H. A review of vessel extraction techniques and algorithms. *ACM Comput. Surv.*, 36(2): 81–121, 2004.
2. Boykov, Y. and Funka-Lea, G. Graph cuts and efficient d-D image segmentation. *Int. J. of Computer Vision*, 70(2): 109–131, 2006.
3. Frangi, A.F., Niessen, W.J, Vincken, K.L., Viergever, M.A. Multiscale Vessel Enhancement Filtering. *LNCS 1496*: 130–137, 1998
4. Ning, X., Narendra, A. and Ravi, B. Object segmentation using graph cuts based active contours. *Computer Vision and Image Understanding*, 107(3):210–224, 2007.
5. Heimann, T. et al., 3D Segmentation in the Clinic: A Grand Challenge I, *MICCAI'07 workshop*. <http://www.sliver07.org>

Robotically assisted minimally invasive aortic valve replacement under MRI guidance

D. Mazilu¹, M. Li¹, A. Kapoor¹, K. Horvath¹

¹National Institutes of Health, National Heart, Lung, and Blood Institute, Bethesda, USA

Keywords Transapical aortic valve repla · Real-time MRI-guided intervent · MRI compatible robot

Purpose

Minimally invasive procedures for aortic valve replacement have emerged as an alternative for open heart aortic valve surgery. The two methods are currently being investigated for minimally invasive aortic valve replacement; a transfemoral and a transapical approach. The catheter based transfemoral method is less invasive but precise placement of a prosthesis by manipulating a long guide wire under x-ray imaging can be a difficult task. The transapical method is more invasive but offers advantages of the shorter distance to the target area and better control of prosthesis placement. Magnetic Resonance Imaging (MRI) provides high resolution images of cardiovascular anatomy without contrast or radiation. Use of real-time MRI (rtMRI) allows physicians to monitor the progress of the procedure and also provides the ability to immediately assess the results, such as ventricular and valvular function, and myocardial perfusion. Our team has performed successful aortic valve replacements in a large animal model using the transapical approach under MRI guidance. Exact placement and orientation in a beating heart in an MRI scanner is a complicated task because of limited space for precise device manipulation. In order to improve accuracy and dexterity, we developed a robotic system for aortic valve replacement under MRI guidance and we report our first ex-vivo results.

Methods

The developed robotic system is fully MRI compatible, and consists of a 3-DOF valve delivery module and a passive or active positioning arm along with the control system. The 3-DOF valve delivery module is comprised of two components: a sterile disposable valve delivery device, and an active manipulation mechanism. The manipulation mechanism provides the ability to appropriately align the valve delivery device for a precise prosthetic valve placement. Pneumatic actuators and an optical encoder are used for moving and positioning each stage of the delivery module. A PIV (proportional position loop integral and proportional velocity) controller is used for servoing the pneumatic valve delivery module movement. To test the accuracy of bioprosthetic valve placement, a phantom that mimics the native aorta (Fig. 1) was developed. The phantom consists of a plastic tube with 25 mm inside diameter mounted on one interior side of a $200 \times 100 \times 100$ mm water tank and a spherical holed joint mounted on the opposite side of the tank. This spherical joint serves as the heart apical insertion point. A standard 5–12 mm trocar was inserted into the spherical joint, and the disposable valve delivery device was inserted

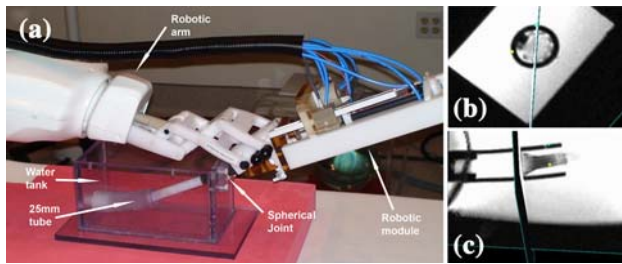


Fig. 1 **a** Robotic system with the phantom setup. **b** short axis view of real-time MR imaging on a self-expanding stent. **c** long axis view of real-time MR imaging on a self-expanding stent

in through the trocar. The trocar and delivery device were mounted on the valve delivery module, and this module was attached to a robotic arm. The bioprosthetic valves were placed in the phantom's aortic annulus using the robotic system under rtMRI guidance. A clinically standard St. Jude bioprosthetic valve was affixed on a custom made self-expanding stent. To verify the correct position and orientation of the bioprosthetic valve a passive marker was affixed on the distal end of the stent. The error placement of the bioprosthetic valve, using our robotic system was studied on a 1.5 T Siemens Espree scanner. A true fast imaging with steady state precession (trufi) scanning sequence was used with following parameter: TR = 3.51 ms, TE = 1.76 ms, imaging flip angle = 45°, slice thickness = 6 mm, field of view (FOV) = 340 × 283 mm, and matrix = 192 × 144. This protocol was similar to the one we used in MR scanning for real time manual transapical aortic valve replacement.

Results

The placement error of the prosthetic valve was defined as the distance between the distal end of the stent and the end of the 25 mm tube. The maximal in-plane displacement error over 10 trials was ± 1.8 mm. The angular error was defined by the angular difference between the line that goes through the center of the tube and the center of the hole that mimics coronary ostia, and the line that goes through the center of the stent and the center of the passive marker. The maximal calculated angular error was $\pm 2.3^\circ$. These errors are cumulate errors of the robotic system and MRI image. The mechanical accuracy of our robotic module was determined on the previous experiments; was found to be 0.19 ± 0.14 mm in linear movement and $0.46 \pm 0.27^\circ$ in rotary movement. The majority of the error is due to slight variations in the real-time MR images.

Conclusion

We have developed and evaluated an MR compatible robotic system to remotely perform transapical aortic valve replacement under MRI guidance. Preliminary results in ex-vivo experiments demonstrate that the robotic system can provide sufficient capabilities to successfully perform precise positioning of a prosthetic aortic valve on a self-expanding stent into a beating heart under MRI guidance. The presence and motion of the robotic system inside the MRI scanner was found to have no noticeable disturbance in the image. Our immediate goal is to evaluate this system in a large animal study.

Automated soft tissue manipulation with mechatronic assistance using endoscopic Doppler guidance

S. Jacobs¹, V. Falk¹

¹University Hospital Zürich, Clinic for Cardiovascular Surgery, Zürich, Switzerland

Keywords Robot surgery · Image guidance · Ultrasound

Objective

The use of intra-operative imaging provides updated information in order to perform finer, more challenging interventions. It is advantageous to assist the surgeon by performing semi-automatic image-

guided instrument control and allow the surgeon to concentrate on more important aspects. The surgeon is released from some simple and repetitive tasks which in turn increases his situational awareness and produces an improvement of the human factors, as well as of the patient safety. In fields such as interventional radiotherapy or spine surgery, intra-operative imaging is used on a regular basis for semi-automatic control of instruments. To demonstrate the applicability of this semi-automatic approach in cardiovascular surgery, a system called ASTMA is built. It consists of a new universal robot with a monopolar blade electrode and an ultrasound probe mounted on it. The robot acts autonomously under the surgeon's supervision and should be able to follow the left internal thoracic artery (LITA) and take it down using intraoperative ultrasound Doppler images. This paper describes the construction of an anterior chest wall phantom that will be used to evaluate the ASTMA system. It replicates the patient's thorax conditions and morphology during the LITA harvesting phase in a classic coronary artery bypass grafting (CABG) intervention

Methods

We build and evaluate a system, consisting of an endoscopic ultrasound probe combined with a monopolar cautery unit, mounted on universal medical robot. The system worked semi-automatically regarding speed and depth control by human. The anatomical structures of a human thorax were divided into three parts: thorax framework, vascular system and surrounding tissue of the LITA. The evaluation set-up of the phantom is shown in Fig. 1. For the thorax framework two 3D models (left, right) were printed out applying the 3D Rapid Prototyping Technology. The vascular system includes the LITA itself and the blood flow. Distilled water was mixed with a silicon antifoaming emulsion to increase the Doppler signal of this blood-like solution. The pumping system generated different flow patterns. The surrounding tissue of the LITA was made of poly-vinyl alcohol (PVA) cryogel. Five subjects were asked to detect the vessel in a 3D phantom model using the Doppler guided robot arm.

Results

In the 3D phantom model the LITA was easily detected from the subclavian artery to the bifurcation from all subjects in $2 \text{ min} \pm 1.3$. In a second run the pedicle was marked with a safety distance of 10 mm for the IMA take down with the cautery. In the first model the expected haptic and echogenic properties were achieved. Figure 2 shows the Axial color Doppler image taken from the phantom obtained from the phantom's vascular system. Face validity tests and ultrasound measurements indicate the feasibility of the phantom design. It was assessed as good by the experts, considering its purpose. This, to our best knowledge, is the first time that plaster, silicon,



Fig. 1 3D Phantom Model including thorax framework, vascular system and surrounding tissue of the LITA and an universal robot with a monopolar blade electrode and an ultrasound probe mounted on it

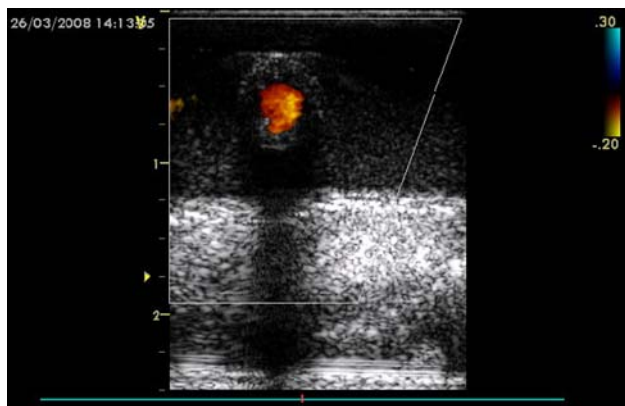


Fig. 2 Axial color Doppler image of the vascular system

and PVA have been combined to create a phantom to evaluate robot-assisted LITA harvesting in classic CABG interventions.

Conclusions

This setting works semi-autonomously to control the alignment of the surgical instrument based on intra-operative images. The task is shared between the surgeon and the robot. This concept of shared autonomy has neither been developed nor applied before to image-guided surgery

3D ultrasound for catheter ablation guidance in the left atrium

A.B. Koolwal¹, F. Barbagli¹, C.R. Carlson², D.H. Liang¹

¹Stanford Univ., CA, USA

²Hansen Medical, Mountain View, CA, USA

Purpose

The catheter ablation procedure is a minimally invasive surgery used to treat atrial fibrillation. Difficulty visualizing the catheter inside the

left atrium anatomy has led to lengthy procedure times and limited success rates. In this paper, we present a set of algorithms for reconstructing 3D ultrasound data of the left atrium in real-time, with an emphasis on automatic tissue classification for improved clarity surrounding regions of interest.

Methods

Using an intracardiac echo (ICE) ultrasound catheter, we collect 2D-ICE images of a left atrium phantom from multiple configurations, and iteratively compound the acquired data into a 3D-ICE volume. We introduce two new methods for compounding overlapping US data—Occupancy-Likelihood and Response-Grid Compounding—which automatically classify voxels as “occupied” or “clear,” and mitigate reconstruction artifacts caused by signal dropout. Finally, we use the results of an ICE-to-CT registration algorithm to devise a Response-Likelihood Weighting scheme, which assigns weights to US signals based on the likelihood that they correspond to tissue-reflections.

Results

Our algorithms successfully reconstruct a 3D-ICE volume of the left atrium with voxels classified as “occupied” or “clear,” even within difficult-to-image regions like the pulmonary vein openings. We are robust to dropout artifact that plagues a subset of the 2D-ICE images, and our weighting scheme assists in filtering out spurious data attributed to ghost-signals from multi-path reflections.

Conclusion

By automatically classifying tissue, our algorithm precludes the need for thresholding, a process that is difficult to automate without subjective input. Our hope is to use this result towards developing 3D ultrasound segmentation algorithms in the future.